NINTH INTERNATIONAL SYMPOSIUM ON "APPLICATIONS OF LASER TECHNIQUES TO FLUID MECHANICS"
JULY 13-16, 1998, THE CALOUSTE GULBENKIAN FOUNDATION, LISBON, PORTUGAL

A NON-NEWTONIAN TURBULENT SUDDEN EXPANSION FLOW

A. S. Pereira
Departamento de Engenharia Química, Instituto Superior de Engenharia do Porto
Rua de S.Tomé, 4200 Porto CODEX, Portugal

F. T. Pinho
Departamento de Engenharia Mecânica e Gestão Industrial
Faculdade de Engenharia, Rua dos Bragas, 4099 Porto CODEX, Portugal

ABSTRACT

A miniaturised fibre optic Laser-Doppler anemometer was used to carry out a detailed hydrodynamic investigation of the flow downstream a sudden expansion with 0.1% to 0.2% by weight shear-thinning aqueous solutions of xanthan gum.

Upstream of the sudden expansion the pipe flow was fully-developed and the xanthan gum solutions exhibited drag reduction with the corresponding lower radial and tangential normal Reynolds stresses, but a higher axial Reynolds stress near the wall and a flatter axial mean velocity profile.

The recirculation bubble length was reduced by more than 20% relative to the high Reynolds number Newtonian flow, and this was attributed to the higher levels of maximum turbulence and their earlier occurence in space for the non-Newtonian solutions. This happened as a result of the advection of the upstream inlet condition leading to both higher initial values of axial turbulence in the free shear layer and higher turbulence production.

1. INTRODUCTION

The vast majority of turbulent flow research with non-Newtonian fluids has concentrated on understanding wall-dominated flows with polymer solutions and more recently surfactants (Gyr and Bewersdorff, 1995), but a better knowledge of turbulent flow behaviour requires also the investigation of wall-free flows, preferably with the same fluids. The axisymmetric sudden expansion flow is easily implemented for liquid flows of non-Newtonian fluids and has been investigated in the past by a few researchers. Pak et al (1990,1991) showed the influences of fluid viscosity and elasticity on the mean flow characteristics or Carbopol and Separan solutions under laminar, transitional and turbulent flow conditions, but failed to report detailed turbulent measurements in the latter case. More recently, Castro and Pinho (1995) have mapped the mean and turbulent fields in the sudden expansion flow of weakly elastic 0.4% and 0.5% by weight aqueous solutions of Tylose (molecular weight of 6,000 kg/kmole), which were previously investigated by Pereira and Pinho (1994) on their fully-developed turbulent pipe flow chracteristics. These solutions were found to be inelastic in conventional rheometric shear tests, but showed drag reductions of less than 24% and 27% in turbulent pipe flow, respectively. In the sudden expansion flow they yielded small variations in the recirculation bubble length and reductions of the normal Reynolds stresses of up to 30%, especially in the tangential and radial directions.

The extension of this research to other fluids exhibiting a higher degree of elasticity in shear rheological flows, and higher levels of drag reduction in turbulent pipe flow, such as the axial solutions of xanthan gum tested by Escudier et al (1995) or the CMC solutions of Pinho and Whitelaw (1990), are deemed necessary to enhance our understanding of turbulent flows of polymer solutions and constitutes the objective of the present work.

In the next section the rig and instrumentation are described, and that is followed by the presentation and discussion of results. The characteristics of the fluids are presented before the hydrodynamic results and the paper ends with a summary of the main conclusions

2. EXPERIMENTAL SET UP

The flow configuration is similar to that used in the pipe flow experiments of Pereira and Pinho (1994) except for the test section and the ensuing duct leading to the tank. The installation consisted of a vertical closed loop with a 100 litre tank and a centrifugal pump located at the bottom. The descending pipe before the test section was 26 mm in diameter and more than 90 diameters long, leading to a transparent sudden expansion test section from 26 mm to 40 mm in diameter and 700 mm in length. Downstream of the test section there is a further pipe of 40 mm diameter which is fitted with a valve and leads the flow to the tank. The test section is represented schematically in Fig. 1 with the coordinate system and it had a square outer cross section to reduce diffraction of light beams.To help ensure a fully developed flow at the inlet of the sudden expansion , a honeyconb was placed at the inlet of the descending 26 mm pipe, i.e., 90 diameters upstream of the sudden expansion plane.

Fourteen pressure taps were located in the pipe downstream of the sudden expansion and two taps were drilled upstream, in the region of fully-developed flow. One of the upstream taps was drilled in the perspex test section whereas the other was located in the brass pipe. The rising

pipe had an electromagnetic flowmeter and two valves which, together with a bypass circuit, allowed the flow rate to be properly monitored. The connection between the brass pipe and the test section was well done and within the machining tolerances of ± 10 μm, causing no detectable harm to the flow condition.

The pressure drop in the sudden expansion was measured by means of differential pressure transducers from Validyne (models P305D) and its output was sent to a computer via a data acquisition board Metrabyte DAS-8 interfaced with a Metrabyte ISO 4 multiplexer, both from Keithley. The overall uncertainty of the pressure measurements varied between 1.6% and 7.2% for high and low pressure differences, respectively.

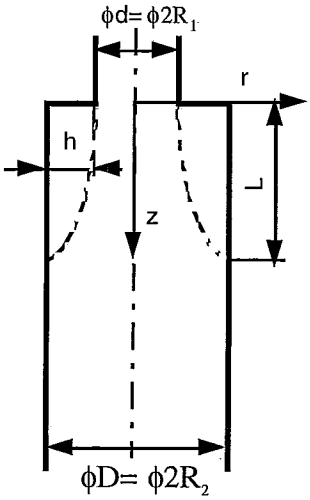

Fig. 1 - Schematic representation of the sudden expansion test section.

Table I - Laser-Doppler characteristics

Laser wavelength	827 nm
Laser power	100 mW
Measured half angle of beams in air	3.68
Size of measuring volume in water (e^{-2} int.)	
minor axis	37μm
major axis	550μm
Fringe spacing	6.44μm
Frequency shift	2.5 MHz

For the velocity measurements a miniaturised fiber optics laser-Doppler velocimeter from INVENT, model DFLDA, similar to that described by Stieglmeier and Tropea (1992), was used, with a 100 mm front lens mounted onto the 30 mm diameter probe. Scattered light was collected by a photodiode in the forward scatter mode, and the main characteristics of the anemometer are listed in Table I and described by Stieglmeier and Tropea (1992). Measurements of the radial velocity component were limited to the inner 70% of the pipe radius due to excessive refraction of light beams outside that region.

The signal was processed by a TSI 1990C counter interfaced with a computer via a DOSTEK 1400 A card, which provided the statistical quantities. The data presented in this paper have been corrected for the effects of the mean gradient broadening and the maximum uncertainties in the axial mean and rms velocities at a 95% confidence level are of 1.0% and 2.2% on axis respectively, and of 1.1% and 5.2% in the wall region. The uncertainty of the radial and tangential rms velocity components is 2.5% and 5.9% on axis and close to the wall, respectively.

The velocimeter was mounted on a milling table with movement in the three coordinates and the positional uncertainties are of ± 200 μm and ± 150 μm in the axial and transverse directions, respectively.

3. FLUID PROPERTIES

Water and aqueous solutions of xanthan gum grade Keltrol TF from Kelco, a polysaccharide of high molecular weight ($2*10^6$ kg/kmol), at weight concentrations of 0.1% and 0.2% were used. This additive produced solutions of higher elasticity than those of CMC of Pinho and Whitelaw (1990) and Tylose of Castro and Pinho (1995), but at the same time the solutions were more shear-thinning, especially at low shear rates. The polymer was dissolved in Porto tap water and 0.02% by weight of the biocide Kathon LXE from Rohm and Haas was added to help prevent bacteriological degradation. The rheological characterisation was carried out in the Physica MC100 rheometer implementing a double gap concentric cylinder geometry.

The viscometric viscosity of the solutions are plotted in Fig. 2 together with the curve-fitted Sisko model equation (Eq. 1), whose parameters are listed in Table II.

$$\eta = \eta_{ref}\left(\lambda_s \dot{\gamma}\right)^{n-1} + \eta_{\infty} \qquad (1)$$

Table II- Sisko model parameters for Keltrol solutions at 25°C.

Solution	η_{ref} [Pas]	η_{∞} [Pas]	λ_s [s]	n
0.1%	10.52	0.0012	1970	0.4299
0.2%	58.06	0.001589	1900	0.3434

To assess the elasticity of the solutions creep and oscillatory tests were carried out. In the creep tests the ratio of the stored shear deformation to the total deformation of the 0.1% and 0.2% xanthan gum solutions was less than 0.04% and 0.15%, respectively for a range of applied stresses between 0.3 and 3 Pa. In the oscillatory shear tests it was not possible to get reliable data for amplitudes of deformation below 0.2. For this amplitude of deformation the ratio of the storage to the loss moduli G'/G'' was less than 0.7 for the 0.1% solution and about 1 for the 0.2% solution.

In spite of the low elasticity shown in the rheological tests, these two solutions exhibited drag reduction in turbulent pipe flow as shown in Fig.3 . In a pipe of 26 mm and for maximum wall Reynolds numbers of 40,100 and 28,100, the measured drag reductions of 45% and 59% for the 0.1% and 0.2% xanthan gum solutions represent over1/2 and 3/4 of the maximum predicted by Virk's asymptote (Virk et al, 1970). Note that these values are substantially higher than those reported by Pereira and Pinho (1994) for identical concentrations of Tylose, but are similar to those of Pinho and Whitelaw (1990) for identical concentrations of CMC.

4. RESULTS AND DISCUSSION

Five flow conditions were investigated in detail and allowed the analysis of the effects of Reynolds number and additive concentration. The Reynolds number Re is defined on the basis of the upstream pipe flow characteristics such as the upstream bulk velocity and wall viscosity. However, for the sake of comparisons with other works in the literature, a generalised Reynolds number (Eq. 2) is also recorded in Table IV which lists the main characteristics of the investigated flows.

$$\mathrm{Re}_{gen} = \frac{\rho D_1^n U_1^{2-n}}{K} \qquad (2)$$

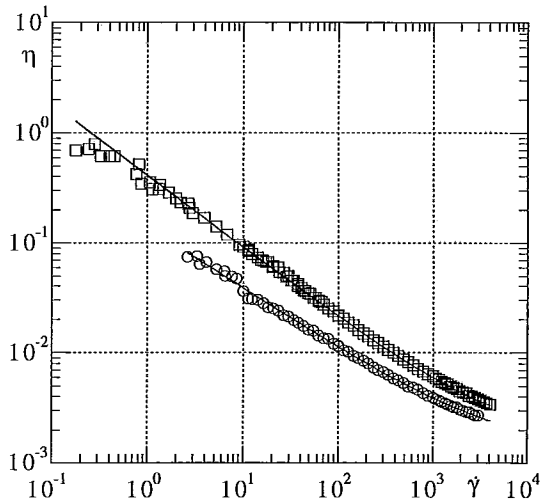

Fig. 2- Viscometric viscosity of the xanthan gum solutions and the corresponding curve fitted Sisko models. O 0.1% Xanthan gum, □ 0.2% Xanthan gum.

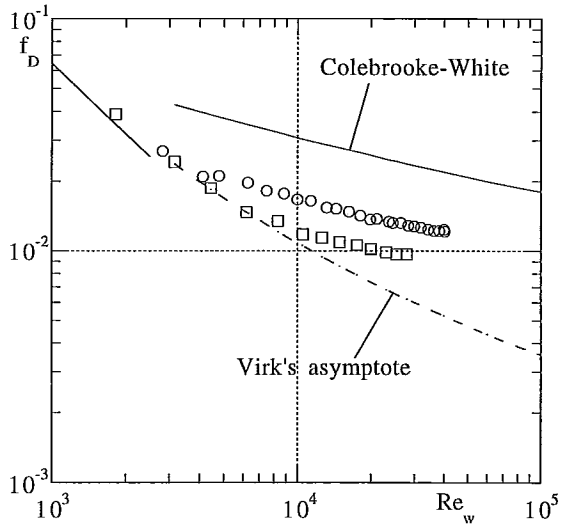

Fig. 3- Darcy friction factor as a function of the wall Reynolds number in a fully developed pipe flow. O 0.1% Xanthan gum, □ 0.2% Xanthan gum.

Note that Eq. (2) requires the power index n and consistency index K of the Ostwald de Waele power law fit to the measured viscosity .

The largest Reynolds number Re flows in Table IV correspond to the maximum flow rate in the rig. The Table lists also the recirculation length L normalised by the step height h. To measure the recirculation length the axial velocity was measured twice in a fine grid around the estimated location of flow reattachment and the data interpolated. The nodes of this grid were spaced axially and radially by 3 mm and 0.2 mm, respectively and the overall uncertainty of the eddy size measurement, due to positional and mean velocity uncertainties, is better than 5%.

Table IV- Main flow characteristics of the investigated flows of water and xanthan gum (XG)

Run	Fluid	Re	Re_{gen}	L/h
1	water	133,000	133,000	8.64
2	water	50,000	50,000	8.47
3	0.1% XG	19,300	7,950	6.61
4	0.2% XG	26,600	10,380	6.42
5	0.2% XG	19,100	7,530	6.64

4. 1. Mean flow

The mean flow measurements showed the flow field in all cases to be similar in that we could identify a core flow, a free shear-layer downstream of the upstream wall pipe, a recirculation region delimited by the step, the downstrream pipe wall and the shear layer, a reattachment region and a redeveloping boundary layer, in accordance to the flow field definition of Pronchick and Kline, (1983).

Our measurements with water compare well in all respects with data from the literature pertaining to Newtonian fluids. In particular the normalised recirculation lengths plotted in Fig. 4 are in good agreement with data from other researchers, especially the values measured by Khezzar (1985), although a small expansion ratio effect in the slightly normalised eddy sizes for the lower expansion ratios is observed. Note also that the values are very similar to those measured by Castro and Pinho in 1995.

Quite unexpected, considering previous non-Newtonian measurements from the literature, is the shorter recirculation observed with the xanthan gum solutions. To the authors knowledge there has been only two investigations of this quantity and their results, together with the present measured lengths, are plotted in Fig. 5. So far it was thought that polymer solutions of non-Newtonian rheology would exhibit unchanged or longer eddy sizes in comparison to the Newtonian values, at identical Reynolds numbers, but this work shows that shorter bubbles can also occur.

As we shall see below the different behavior can be explained by the turbulent flow field, especially by the location and magnitude of the maximum normal Reynolds stresses. However, before analysing in detail the flow downstream of the expansion it is convenient to assess well the inlet flow condition.

Pressure gradients measured between the two upstream pressure taps were in agreement with the measured pressure gradients obtained for the same fluid flow in the pipe flow rig described in Pereira and Pinho (1994). Fig. 6-a) shows the fully developed radial profiles of the mean axial velocity u in the pipe upstream of the sudden expansion. The velocities were normalised by the maximum velocity

and the profiles at higher Reynolds numbers are flatter than those pertaining to lower Reynolds number flows. The mean and turbulent Newtonian velocity profiles are in agreement with those of the literature (Laufer, 1954 and Lawn, 1971), thus confirming a fully developed flow condition at the inlet of the expansion.

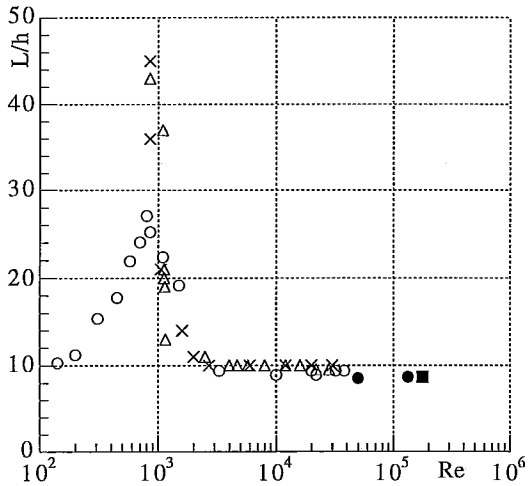

Fig. 4- Normalised recirculation length for Newtonian fluids. O Khezzar (1985) D/d=1.749; X Pak et al (1990) D/d= 2.0; Δ Pak et al (1990) D/d= 2.667; ■ Castro and Pinho (1995) D/d= 1.538; ● Present work D/d= 1.538.

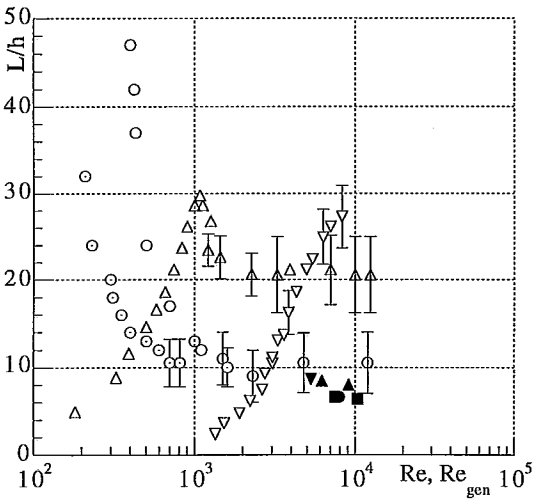

Fig. 5- Normalised recirculation length for non-Newtonian fluids. Pak et al (1990) D/d=2.667: O Carbopol 5000ppm, ⊙ Carbopol 15000 ppm; Pak et al (1990) D/d=2.0: Δ Separan 200 ppm, ∇ Separan 1000 ppm; Castro and Pinho (1995) D/d= 1.538: ▲ 0.4% Tylose,▼ 0.5% Tylose; Present work D/d= 1.538: ● 0.1% Xanthan gum, ■ 0.2% Xanthan gum.

The profiles for the 0.1% Xanthan gum solution at Re= 19,300 and the 0.2% Xanthan gum solution at Re= 26,600 are flatter than any of the Newtonian profiles, in spite of their higher Reynolds numbers. In our view this helps to explain the observed shorter recirculation bubble, as we shall see below.

The non-Newtonian turbulent velocity profiles in Figs. 6-b) to -d) are typical of fluids which exhibit drag reduction. Both transverse turbulence intensities (v' and w') are considerably dampened in relation to that of their Newtonian counterparts, especially when we take into account that a reduction in the Reynolds number in fully-developed pipe flow is equivalent to an increase in the turbulence (compare data for Newtonian flows at Re=50,000 and Re= 131,000). However, the axial turbulence of the xanthan gum solutions is only slightly reduced in the central part of the pipe whereas near the wall the maximum turbulence becomes considerably higher than for Newtonian fluids. This different behaviour means that there is decoupling between the axial and transverse turbulence which explains the reduced friction.

Fig. 7 shows radial profiles of the axial mean velocity at various axial planes downstream of the expansion. Near the expansion (x/d=0.25 to 0.75) the flow of the non-Newtonian solutions have a flatter profile in the core and higher negative velocities within the recirculation region, consequently they exhibit a stronger shear layer. This feature is especially relevant as it contributes to higher turbulence production and higher levels of turbulence in the free shear layer, as will be shown in the next section. It is also worth mentioning that the ratio of the velocity on axis to the bulk velocity increases until about x/D= 0.5 to 1.0, with that effect more pronounced with the Newtonian fluid

As the flow proceeds further downstream the mean velocity of all solutions seem to collapse, but we continue to observe anticipated features for the non-Newtonian flows in space relative to the water flows.

4. 2. Turbulent flow

Table V shows the maximum values of the normalised normal Reynolds stresses and of the turbulent kinetic energy. Note that the maximum normal stresses do not occur at the same location, therefore their sum does not yield the maximum kinetic energy. Everywhere else in the flow field, the axial Reynolds stress is always the highest turbulent stress followed by the tangential and then the radial components.

Table V- Maximum values of the normal Reynolds stresses

Run	$\overline{u^2_{max}}/U_1^2$	$\overline{w^2_{max}}/U_1^2$	$\overline{v^2_{max}}/U_1^2$	k^2_{max}/U_1^2
1	0.0495	0.0324	0.0227	0.0513
2	0.0440	0.0271	0.0221	0.0480
3	0.0417	0.0312	0.0195	0.0461
4	0.0552	0.0337	0.0242	0.0556
5	0.0470	0.0333	0.0225	0.0505

It is clear that a reduction of the Reynolds number, at low Reynolds numbers, leads to lower maximum turbulence whereas an increase in polymer concentration increases it. For instance, the 0.2% xanthan gum at Re of 26,600 has maximum values of the axial Reynolds stress 10% higher than that of the water flow at Re of 133,000 and about half that for the other two components of turbulence.

The whole turbulent flow field is shown in the contour plots of the normalised axial, tangential and radial normal Reynolds stresses of Figs. 8, 9 and 10, respectively.. At first look the various plots look identical, but closer inspection shows the following differences: the non-Newtonian solutions develop the maximum Reynolds stresses earlier in space than the Newtonian flows and for some cases those quantities attain higher values as pointed out above. Then, on moving downstream the Reynolds stresses of the non-Newtonian solutions decay at a faster rate than those of the Newtonian flows, and this is particularly clear for the radial, and less so for the tangential components. Some of these differences could be better observed with x-y plots but these had to be ommitted for reasons of space.

Initially we would think that a stronger turbulence dampening of the Reynolds stresses of these drag reducing, non-Newtonian fluids would lead to longer recirculation lengths, a result which would agree with the literature data in Fig. 5, but instead a reduction in eddy size was measured.

The mean and turbulent velocity plots show that the xanthan gum solutions initially develop turbulence in the shear layer at a faster rate than the Newtonian flows, and reach higher values of the maximum Reynolds stresses, whereas the strong dampening of turbulence, especially of its transverse components, becomes effective in lowering the Reynolds stresses below the Newtonian level at the end of the reattachment and in the flow redevelopment regions only. This pronounced effect of the polymer additive upon tranversal turbulence has been observed before in sudden expansion free-shear layers with Tylose solutions (Castro and Pinho, 1995) and in jets with polyacrilamide and polyethylene oxide solutions (Berman and Tan, 1985) and is also typical of wall dominated turbulent flows.

This apparent contradiction is explained as follows: the faster increase of turbulence in the free shear layer observed with the xanthan gum solutions is consistent with differences measured in the fully-developed pipe inlet condition. The flatter axial mean velocity profiles of the xanthan gum solutions (Fig. 6) lead to higher mean velocity gradients in the free shear layer (Fig. 7). The Reynolds shear stress was not measured but it is expected that in the upstream pipe it will be lower than for the Newtonian fluids because of the axial-transverse turbulence decoupling typi-

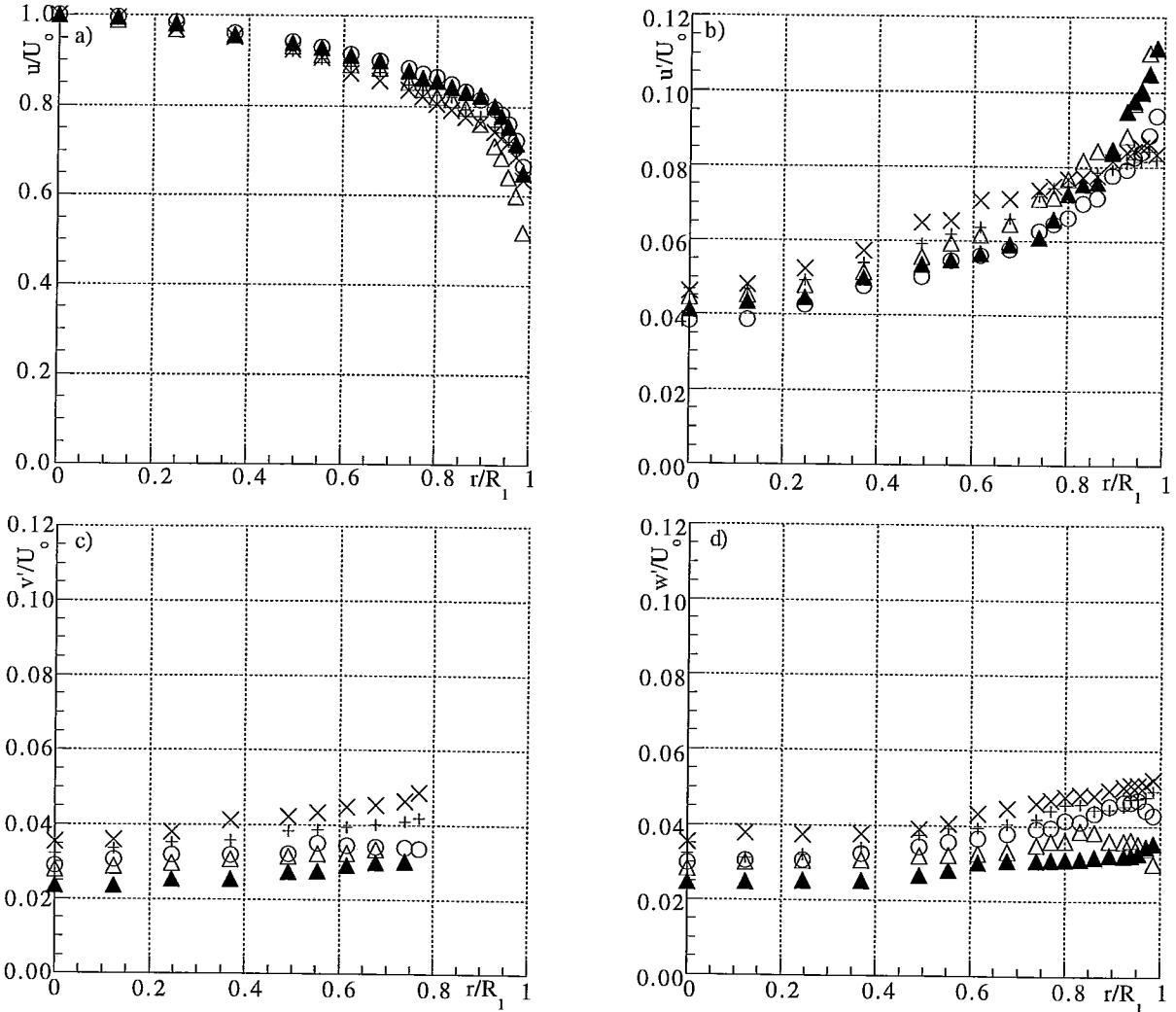

Fig. 6- Radial profiles of normalised mean and turbulent velocities at x/d=0.25 upstream of the expansion. X water Re= 50,000; + Water Re= 131,000 ; O 0.1% Xanthan gum Re_w= 19,300; Δ 0.2% Xanthan gum Re_w= 19,100; ▲ 0.2% Xanthan gum Re_w= 26,600. a) Axial mean velocity; b) Axial rms velocity; c) Radial rms velocity; d) Tangential rms velocity.

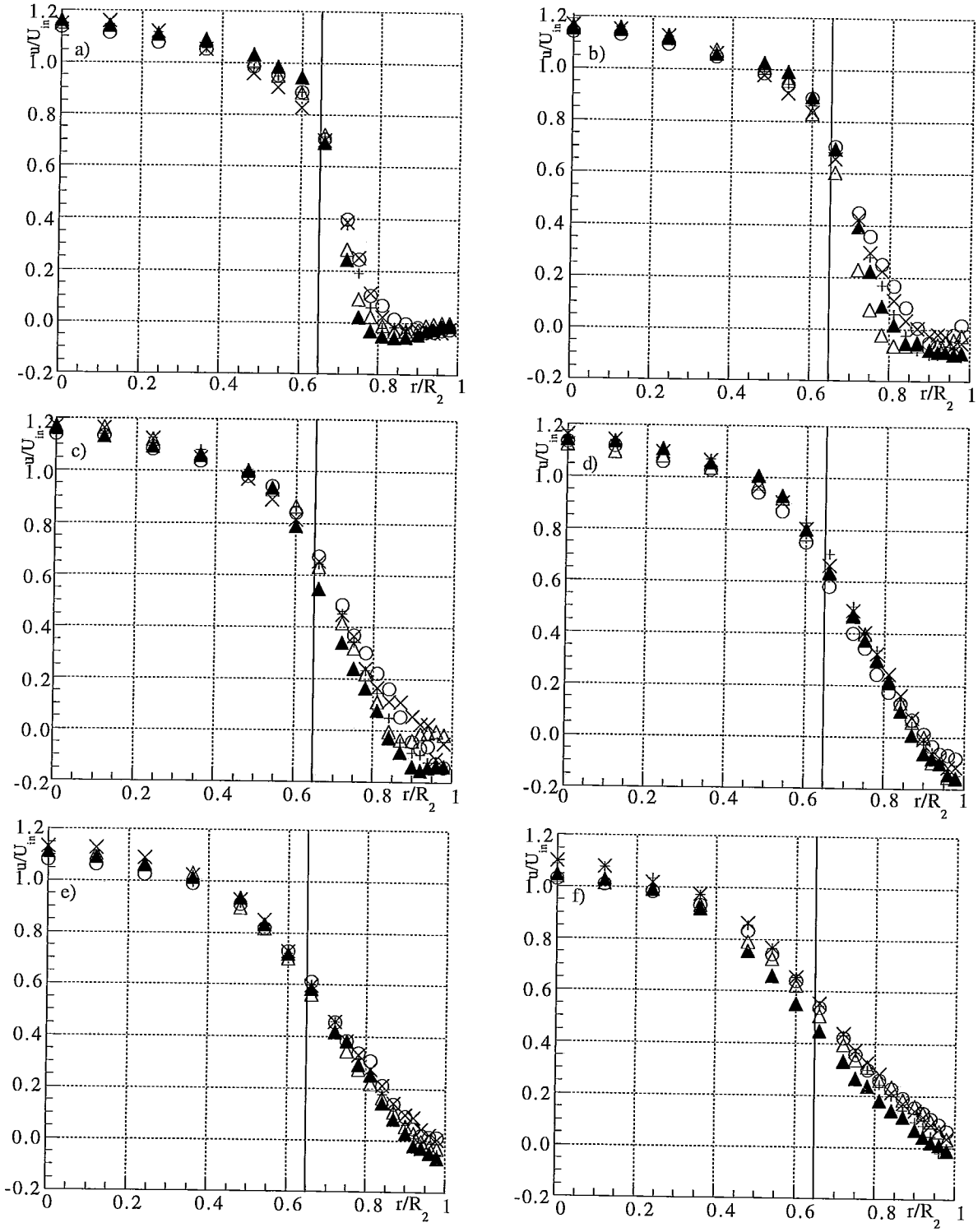

Fig. 7- Radial profiles of normalised mean velocity downstream of the expansion. X water Re= 50,000; + Water Re= 131,000 ; O 0.1% Xanthan gum Re_w= 19,300; Δ 0.2% Xanthan gum Re_w= 19,100; ▲ 0.2% Xanthan gum Re_w= 26,600. a) x/d=0.25; b) x/d=0.5; c) x/d=0.75; d) x/d=1.0; e) x/d=1.5; f) x/d=2.0. Staright line marks the location of the inlet pipe wall.

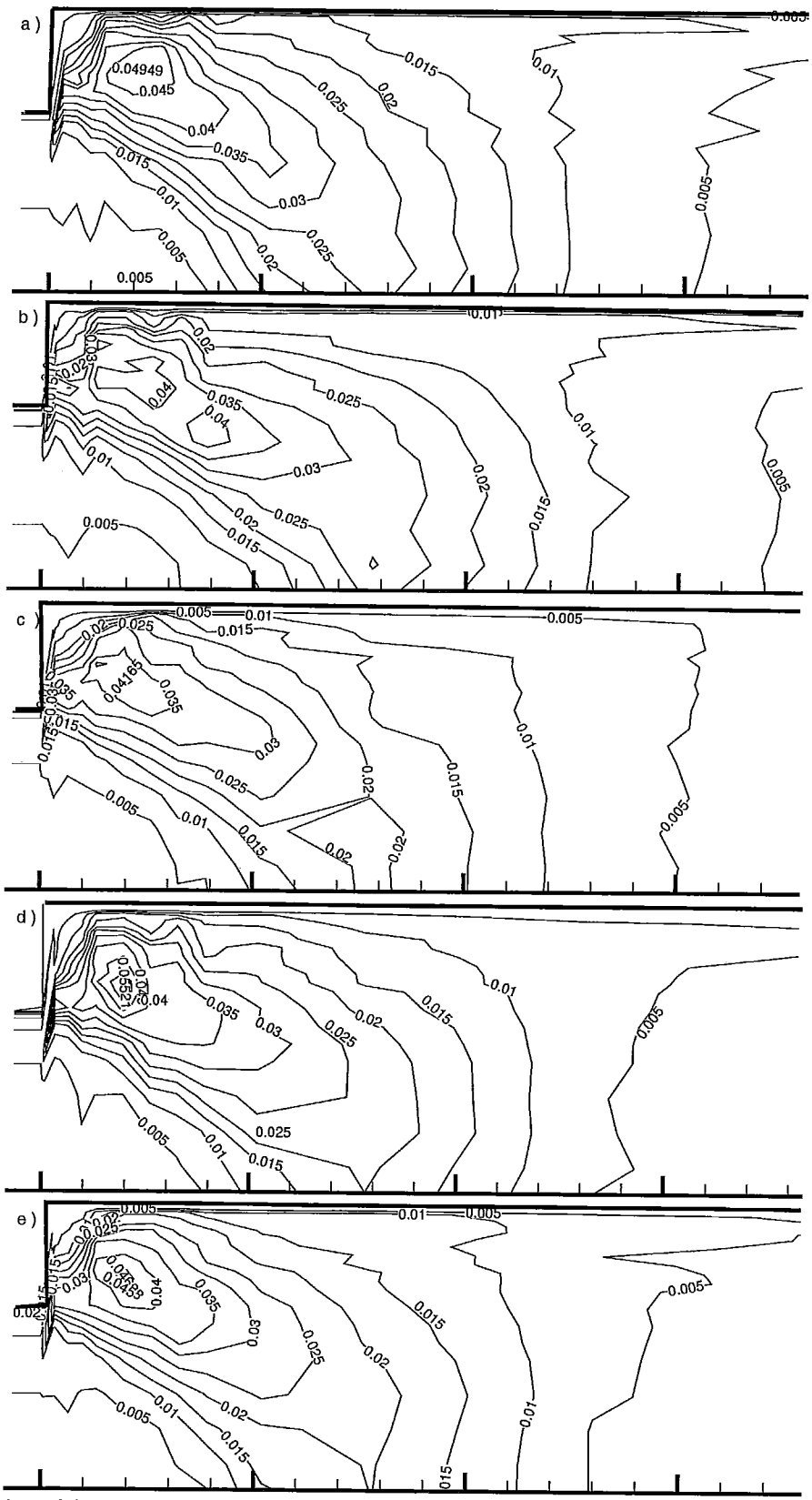

Figs. 8- Countour plots of the normalised axial normal Reynolds stress. a) water Re= 133,000; b) water Re= 50,000; c) 0.1% XG Re= 19,300; d) 0.2% XG Re= 26,600; e) 0.2% XG Re= 19,100.

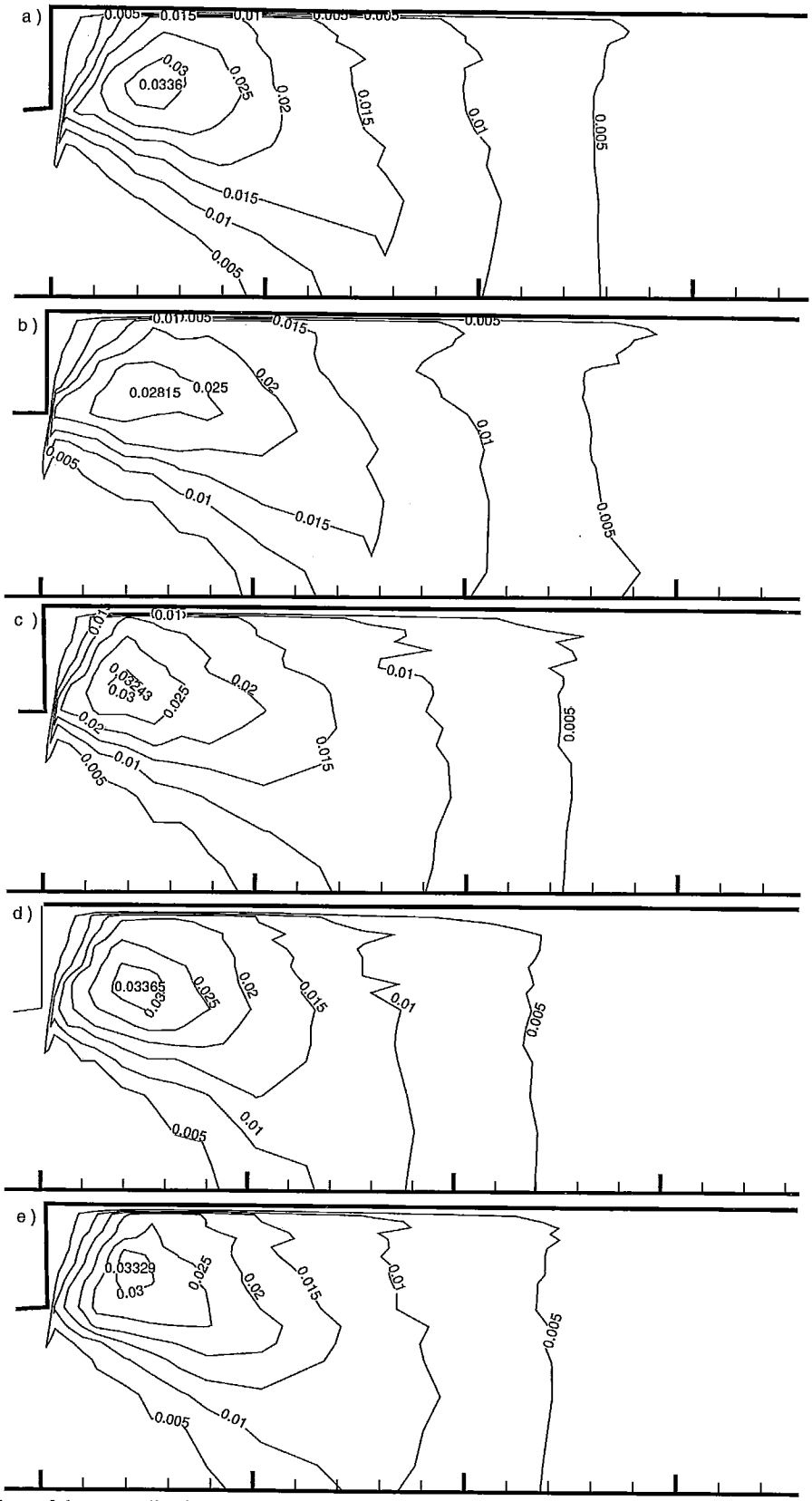

Fig. 9- Countour plots of the normalised tangential normal Reynolds stress. a) water Re= 133,000; b) water Re= 50,000; c) 0.1% XG Re= 19,300; d) 0.2% XG Re= 26,600; e) 0.2% XG Re= 19,100.

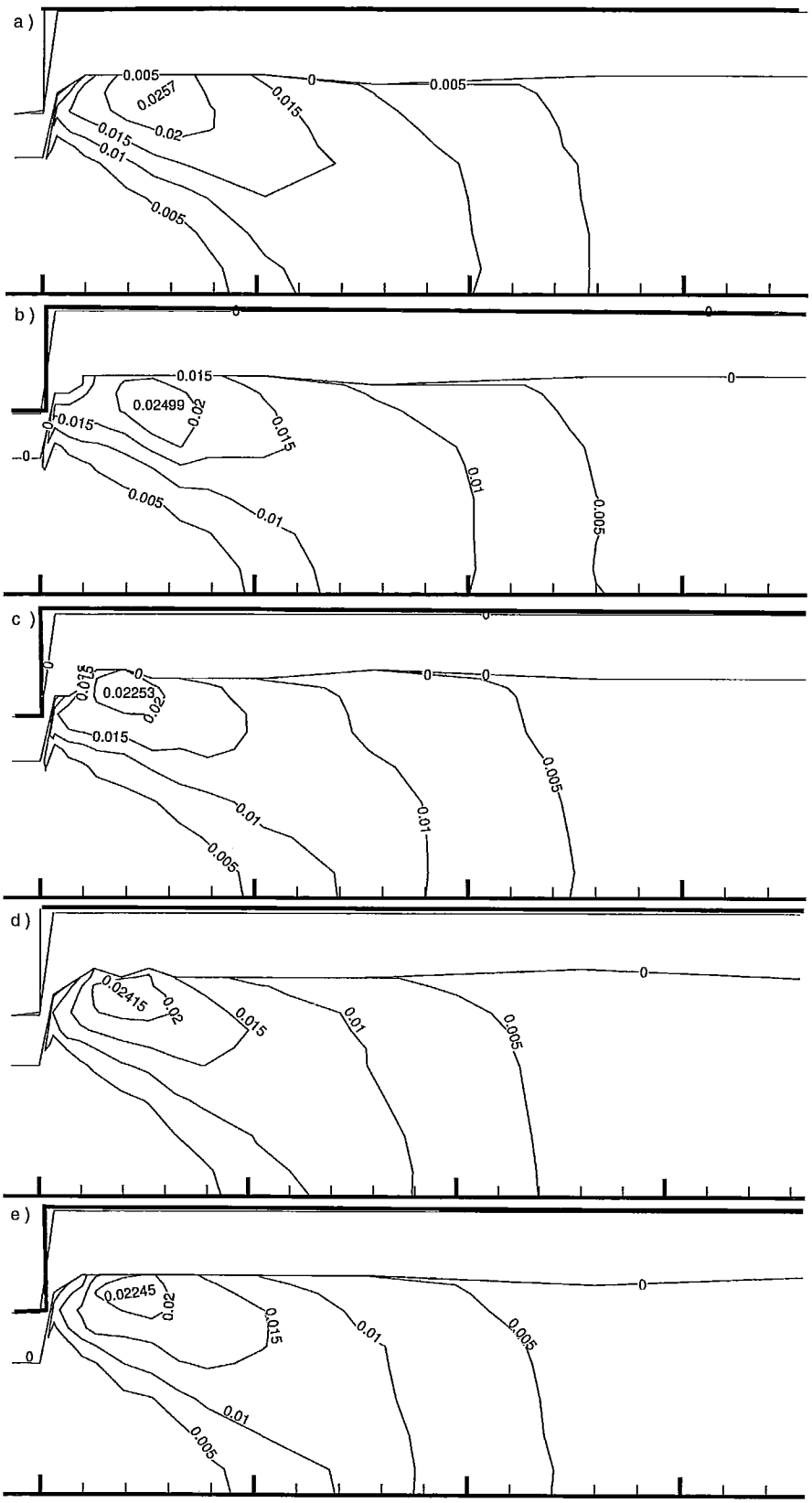

Fig. 10- Countour plots of the normalised radial normal Reynolds stress. a) water Re= 133,000; b) water Re= 50,000; c) 0.1% XG Re= 19,300; d) 0.2% XG Re= 26,600; e) 0.2% XG Re= 19,100.

cal of drag reducing fluids. So, production of $\overline{u_1^2}$

$$\Pr od = \overline{u_1^2}\frac{\partial U_1}{\partial x_1} + \overline{u_1 u_2}\frac{\partial U_1}{\partial x_2} \quad (3)$$

via the second term on the right-hand-side of Eq (3) could be similar to that in Newtonian fluids because of the compensating variations in the shear velocity gradient and shear Reynolds stress. Then, the higher axial turbulence in the wall region of the upstream pipe is advected downstream and should increase the production of $\overline{u_1^2}$ via the first term on rhs of Eq. (3) but, more important, it leads to a higher initial level of axial turbulence in the free-shear layer. The higher maximum values of axial turbulence found in the shear layer for the xanthan gum solutions and its redistribution by the pressure strain also increase the other two normal Reynolds stresses.

The higher levels of turbulence in the middle of the shear layer enhance momentum transfer to the downstream pipe wall region, thus reducing the eddy size.

Further research with different polymer additives, inlet conditions and expansion ratios are deemed necessary to a full and comprehensive understanding of this type of flows for non-Newtonian solutions.

5. CONCLUSIONS

Measurements of the mean and turbulent flow fields downstream a sudden expansion were carried out for a Newtonian and two elastic xanthan gum aqueous solutions at Reynolds numbers between 19,000 and 133,000.

Addition of polymer resulted in drag reduction in the upstream pipe flow which was characterised by flatter axial mean velocity profiles and higher axial normal Reynolds stresses in the wall region which was then advected downstream by the mean flow. These resulted in enhanced velocity gradients and higher axial turbulence in the shear layer downstream of the expansion plane, thus increasing turbulence production. The maximum values of normal Reynolds stresses pertained to the non-Newtonian solutions and the eddy size was reduced by a factor of 20% relative to the water flows.

ACKNOWLEDGEMENTS

The authors would like to thank the financial support of the Stichting Fund of Schlumberger, of project PBIC/CEG/2427/95 of the Portuguese Research Council JNICT and the laboratories of INEGI- Instituto de Engenharia Mecânica e Gestão Industrial- where the whole work was carried. The authors are listed alphabetically.

REFERENCES

Berman, N. S. and Tan, H. 1985. Two-component Laser-Doppler Velocimeter Studies of Submerged Jets of Dilute Polymer Solutions. A. I. Ch. E. J., vol. 31, pp 208-215.

Castro, O. S. , and Pinho, F. T. 1995. Turbulent Expansion Flow of Low Molecular Weight Shear-Thinning Solutions. Exp. in Fluids, vol. 20, pp. 42-45.

Escudier, M. P., Gouldson, I. W., and Jones, D. M. 1995. Flow of Shear-Thinning Fluids in a Concentric Annulus., Exp. in Fluids, vol. 18, pp 225-238.

Gyr, A. and Bewersdorff, H.- W. 1995. Drag reduction of turbulent flow by additives. Fluid Mechanics and Its Application Series, Kluwer Academic Publishers.

Khezzar, L. 1985. An experimental study of flows through round sudden expansions. Imp. College of Science and Technology, Mech. Eng. Dep., Fluids Section Report, London.

Laufer, J. 1954. The structure of turbulence in fully developed pipe flow. National Bureau of Standards, Report 1154.

Lawn, C. J. 1971. The determination of the rate of dissipation in turbulent pipe flow. J. Fluid Mech., vol. 48, pp 477-505.

Pak, B., Cho, Y. I., and Choi, S. U. S. 1990. Separation and Reattachment of Non-Newtonian Fluid Flows in a Sudden Expansion Pipe. J. Non-Newt. Fluid Mech., vol. 37, pp. 175-199.

Pak, B., Cho, Y. I., and Choi, S. U. S. 1991. Turbulent Hydrodynamic Behaviour of a Drag- Reducing Viscoelastic Fluid in a Sudden Expansion Pipe. J. Non-Newt. Fluid Mech., vol. 39, pp. 353-373.

Pereira, A. S. and Pinho, F. T. 1994. Turbulent Pipe Flow Characteristics of Low Molecular Weight Polymer Solutions. J. Non-Newt. Fluid Mech., vol. 55, pp 321-344.

Pinho, F. T,. and Whitelaw, J. H. 1990. Flow of Non-Newtonian Fluids in a Pipe. J. Non-Newt. Fluid Mech., vol. 34, pp. 129-144.

Pronchick, S. W., and Kline, S. J. 1983. An Experimental Investigation of The Structure of Turbulent Reattachment Flow Behind a Backward- Facing Step, Report MD-42, Thermosciences Div., Mech. Eng. Dept., Stanford University.

Stieglmeier, M. and Tropea, C. 1992. A Miniaturized, Mobile Laser- Doppler Anemometer, Applied Optics , vol. 31, pp. 4096.

Virk, P. S., Mickley, H. S. and Smith, K. A. 1970. The Ultimate Asymptote and Mean Flow Structure in Tom's Phenomena. J. Appl. Mech., vol. 37, pp. 488-493.